

Mechanics of Advanced Composite Structures

Journal homepage: https://macs.semnan.ac.ir/

ISSN: 2423-7043



Research Article

Prediction and Parametric Effect in Drilling of Natural Fiber Laminate Using Combined Taguchi- Artificial Neural Network Approach

Velmurugan Samikkannu a*, Raja Murugan Thavidan Vellaiyan a, Subravel Visvalingam b

^a Department of M<mark>anufacturing En</mark>gineering, Annamalai University, Chidambaram, 608002, India ^b Depart<mark>ment of Mechanical E</mark>ngineering, Government College of Engineering, Thanjavur, 613402, India

ARTICLE INFO

ABSTRACT

Article history:

Received: Revised: Accepted:

Keywords:

Taguchi; artificial neural network (ANN); hand lay-up technique; Surface roughness (SR); Scanning electron microscope (SEM). The study investigates the prediction and parametric effects in drilling of Prosopis juliflora fiber (PJF)-reinforced epoxy resin hybrid composite using a combined Taguchi-artificial neural network (ANN) approach. The composite was prepared via hand lay-up technique with natural reinforcement including vetiver fiber (VF) and coir pith (CP). The effects of drill bit diameter (DBD), spindle speed (SS), and feed rate (FR) on thrust force (TF) and surface roughness (SR) were evaluated through a full factorial design. An ANN model developed using a feedforward backpropagation algorithm successfully predicted the responses. Analysis of variance (ANOVA) results revealed that the regression coefficient (R2) for TF and SR were 96.39% and 95.54%, respectively. The DBD and FR were identified as the most significant parameters influencing TF and SR, both significant at the 95% confidence level (p<0.05). The regression plot exhibited a strong correlation (R=0.9883) between the predicted and actual values, while the ANN model achieved a mean squared error (MSE) of 0.089758 within 2 epochs. TF and SR increased with higher DBD and FR but decreased with an increased SS, as indicated by the main effect plots. Scanning electron microscope (SEM) revealed drillinginduced mechanisms, including fiber pullout, delamination, matrix cracking, matrix debonding, and matrix deformation. The findings demonstrate enhanced machining performance, offering potential for industrial applications and future research on biocomposite materials.

© 2025 The Author(s). Mechanics of Advanced Composite Structures published by Semnan University Press. This is an open access article under the CC-BY 4.0 license. (https://creativecommons.org/licenses/by/4.0/)

1. Introduction

Composite materials are gaining significant attention in diverse engineering applications due to their exceptional characteristics, including high strength-to-weight ratio, corrosion resistance, and remarkable versatility [1]. Natural fiber-reinforced composites have emerged as viable alternatives to conventional synthetic fiber composites, attributed to their eco-friendly behaviour, abundant availability,

and cost-effectiveness [2]. In particular, Prosopis juliflora fiber (PJF), derived from the mesquite tree, has demonstrated promising mechanical properties and is widely explored for its potential applications in composite materials [3]. Epoxy resin is extensively used as a matrix material in composite manufacturing due to its excellent mechanical properties, chemical resistance, and ease of processing. When combined with natural fiber like Prosopis juliflora, epoxy resin binder

E-mail address: velezhil07@gmail.com

Cite this article as:

^{*} Corresponding author.

exhibit enhanced mechanical composites performance, making them ideal for a range of structural applications [4]. A crucial aspect in the practical engineering applications of composite materials is their machinability, particularly drilling behaviour, as it significantly influences manufacturing processes like assembly, fabrication, and quality control. Understanding the drilling behaviour of composite materials is essential for optimizing machining parameters. minimizing tool wear, and ensuring dimensional accuracy of machined components [5]. Despite the growing interest in natural fiber-reinforced epoxy composites, comprehensive studies on the prediction and optimization of performance remain limited [6]. Therefore, this study aims to experimentally investigate the drilling behaviour of various natural fiber reinforced composites through a series of drilling tests.

The PIF is gaining increasing popularity in the field of composite materials, especially when combined with polyester-based binders. Ganesan et al. [7] conducted an experimental investigation on the mechanical behaviour of hybrid composites made from natural fibers, specifically Calotropis gigantea and Prosopis juliflora. Taguchi-Grey Relational analysis was employed to enhance the mechanical properties of the composites. Raja et al. [8] investigated the delamination and drilling behaviour of neem and banyan fiber-reinforced sawdust particles hybrid composite through response surface methodology (RSM). According to an ANOVA test, the optimal drilling parameters were DBD of 6 mm, FR of 10 mm/rev, and SS of 1500 rpm. The minimum TF of 23.43 N and torque of 5.13 N-m was achieved under these conditions. Lilly Mercy et al. [9] studied the drilling behaviour of teak wood reinforced epoxy resin using a Taguchi L9 orthogonal array. The effect of SS and FR on TF and temperature was analysed during the drilling process. The results revealed that as SS increased, TF decreased, and temperature increased. Conversely, as FR increased, TF increased while temperature decreased. Mohan Kumar et al. [10] investigated the drilling characteristics of palmyra sprout fiber natural composite, focusing on drilling parameters such as rotating speed, tool feed, and resin types. The results revealed that the candlestick drill bit produced lower TF compared to twist and step cone drill bits. Rajaraman et al. [11] investigated the drilling parameters for kenaf and banana-based composite materials. They used high-speed steel drill bits of three different diameters, and they employed the L9 factorial method for their experimental study. The results revealed that SS of 3000 rpm and FR of 150 mm/min were optimal for producing defect-free holes. Boga and

Koroglu [12] predicted and optimized machining parameters for enhancing surface roughness in dry milling of high-strength carbon fiber composite using an ANN and a genetic algorithm (GA). ANOVA results revealed that cutting tool and feed rate are the most significant factors in enhancing SR. The best SR was achieved at 250 mm/rev and 5000 rpm with a TiAlN-coated tool, with a correlation value of 0.96177 and a mean square error of 0.074, demonstrating its efficacy in surface roughness estimation and achieving high prediction accuracy. Bolat et al. [13] predicted the milling performance of low-cost expanded clay-added synthetic foam using ANN. The experiments were performed using a 3-axis CNC-based milling machine, with controlled process variables including cutting speed, lubrication condition, and depth of cut. The Levenberg-Marquardt algorithm demonstrated superior performance in predicting milling performance compared to the scaled conjugate gradient method.

The literature findings revealed that a natural fiber-reinforced hybrid composite improves machining behaviour. The Taguchi approach was widely applied in various composite drilling processes, resulting in enhanced machining performance. However, no investigations have been recorded on the optimization and prediction of the drilling process using a combined optimization approach. The TF and SR are critical parameters that significantly influence the quality and efficiency of drilling operations. Hence, it is important to optimize and predict the process during the drilling of natural fiber-reinforced composites. This investigation offers new insights for machining of biocomposites with challenging behavior employing a hybrid Taguchi-ANN method to predict and optimize drilling performance of Prosopis juliflora fiber composite. The problem addressed in this study is to identify the process parameters and their optimal levels to enhance both the drilled surface quality and the performance of the composite.

2. Materials and Methods

In this investigation, Prosopis juliflora fiber (PJF), vetiver fiber (VF), and coir pith (CP) were selected as the natural reinforcement materials, while epoxy resin (LY-5062) and hardener (HY-5062) were chosen as the matrix components. The matrix and reinforcement composition comprised 40% PJF, 25% VF, 13% CP, 14% ER, 6% cobalt, and 2% catalyst.

2.1. Preparation of Fibres and Composites

The extracted natural fibers (PJF, VF, and CP) are dried at room temperature for 3 days and

oven-conditioned at 60°C for 5 hours. Prior to the heat treatment process, the average moisture content of PJF, VF, and CP is maintained at 5.44%, 6.54% and 4.48%, respectively. The extracted natural fiber has been subjected to drying at room temperature and a heat treatment process, as depicted in Fig. 1.



Fig. 1 (a) Fiber extraction, (b) heat treatment

After preparing the fibers, a wooden mold was prepared to fabricate the composite. The matrix for fabricating composite laminates was formulated by blending resin and hardener in a 10:1 weight ratio, respectively. The epoxy resin and hardener mixture were thoroughly blended using a mechanical stirrer for 10 min to ensure uniform consistency before being poured into the mold. The composite laminates were developed using the hand-lay-up method. Initially, the treated natural fibers were carefully arranged in the mold, and matrix material on the fibers. The fibers were again arranged over the matrix materials, and discharged matrix material on the fiber surfaces. A roller was employed to evenly distribute the matrix across the entire area of the mold. To achieve uniform thickness and remove excess matrix materials, the mold was subjected to loads of 10 kg for 12 hours at room temperature. Then, the composite laminate was placed in a hot air oven at 60°C for 1 hour to ensure complete curing. The final fabricated composite laminate is depicted in Fig. 2.



Fig. 2. Composite laminate fabricated in the study

2.2 Drilling Experimental Procedure

The drilling of fabricated laminate was conducted using a vertical machining centre (Model: LV 45, Make: LMW), as shown in Fig. 3, at Research Institute, Coimbatore. The experiment design was planned using Taguchi L27 orthogonal array, incorporating three process parameters and their levels, as detailed in Table 1. Drill bits with varying diameters were used for investigation. As per the experimental design, a total of 27 experiments were conducted on the laminate composite, as illustrated in Fig. 4. For each drill bit, nine experiments were performed, varying the other parameters. The experimental values of TF and SR are listed in the Table. 2. The TF was measured using a dynamometer piezoelectric (Kistler type), mounted on the machining table to record realthrust force during drilling. dynamometer was connected to a acquisition system for continuous monitoring and precise measurement. The SR values were measured using a contact-type surface roughness tester (Mitutoyo SJ-210). For each sample, three measurements were taken for both TF and SR, and the average was considered the experimental result.



Fig. 3. Vertical machining centre

Table 1. Drilling parameters and their levels

Parameter	Unit		Levels		
1 di diffetei	Ome	Low Medium High			
Drill bit Diameter (DBD)	mm	6	8	10	
Spindle speed (SS)	rpm	740	1480	2220	

Feed rate (FR)	mm/min	80	160	240
----------------	--------	----	-----	-----

 $\textbf{Table 2.} \ \textbf{Experimental values of TF and SR}$

	- N	D	rilling Para	Re	sponses		
	Ex. No	DBD (mm)	SS (rpm)	FR (mm/min)	TF (kgf)	SR (µm)	
	1	6	740	80	2.3	6.11	
	2	6	740	160	3.3	7.21	
	3	6	740	240	4.0	8.28	
	4	6	1480	80	3.2	5.21	
	5	6	1480	160	3.8	6.75	
	6	6	1480	240	4.7	7.95	
	7	6	2220	80	2.3	4.56	
700	8	6	2220	160	3.2	6.05	
MA	9	6	2220	240	4.3	7.25	
	10	8	740	80	2.7	7.73	
	11	8	740	160	3.6	8.56	
	12	8	740	240	4.5	9.59	
	13	8	1480	80	3.4	7.12	
	14	8	1480	160	4.5	7.85	
	15	8	1480	240	5.4	8.88	
	16	8	2220	80	2.7	6.14	
	17	8	2220	160	3.6	7.05	
	18	8	2220	240	4.6	7.81	
	19	10	740	80	3.4	8.98	
MA	20	10	740	160	4.3	8.61	
	21	10	740	240	5.3	9.15	
	22	10	1480	80	3.9	9.05	
	23	10	1480	160	4.7	9.68	
	24	10	1480	240	5.8	8.48	
	25	10	2220	80	3.5	7.91	
	26	10	2220	160	4.0	8.18	
	27	10	2220	240	5.1	8.96	
UNGORRA S.I 0.70							



Fig. 4. Drilled laminate composite

2.3 Artificial Neural Network Model

ANN is a computational model designed to process input parameters and generate output responses using predefined activation functions. Commonly referred to as a multilayer perceptron, the ANN serves as an excellent method for connecting process parameters to the response characteristics and predicting outcomes [14]. This technique effectively uncovers complex curvilinear and quadratic relationships across various input levels, even in poorly defined systems [15]. In this study, two responses, such as TF and SR, were investigated, with a proposed ANN to predict their responses. Similar to the human brain, ANNs excel at performing nonlinear tasks by leveraging bias and weight values to model complex relationships. The feedforward backpropagation algorithm was applied in this study to develop the model. The architecture of the ANN model employed in the study is depicted in Fig. 5. The basic structure of an ANN comprises three layers: the input layer, hidden layer, and output layer.

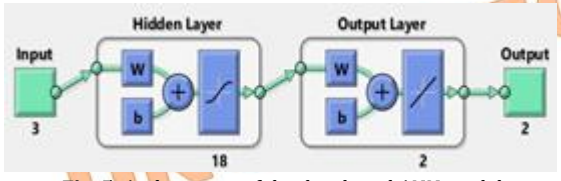


Fig. 5. Architecture of the developed ANN model

In this research, three process parameters, i.e,

DBD, SS, and FR, were used as input. Therefore, the first layer, known as the input layer, consists of three input parameters. The maximum number of neurons is determined based on the learning

rate, which ranges from E-4- E-1. The hidden layer, represented as the middle layer, contains between 18 neurons. The optimal performance of the ANN model is achieved by adjusting its complexity appropriately. When the hidden layer is configured with the optimal number of neurons. the model exhibits improved performance, offering more accurate predictions and well-aligned points along the response curve. However, an overly complex architecture can limit the ability of the model to generalize, potentially leading to overfitting and reduced performance on unseen data. The output variables, represented as the third layer, include two response measures (TF and SR). The data set was randomly split into 80% for training and 10% of data for validation and testing. The formulas for the coefficient of determination (R2) and root mean squared error (RMSE) are given in Equations (1) and (2), respectively, as follows:

$$R^{2} = 1 - \frac{\sum_{i=1}^{n} (y_{i} - \hat{y}_{i})^{2}}{\sum_{i=1}^{n} (y_{i} - \bar{y}_{i})^{2}}$$
(1)

$$MSE = \sqrt{\frac{1}{n}} \sum_{i=1}^{n} (y_i - \hat{y}_i)^2$$
 (2)

where.

 y_i -Actual value of input parameters

 \hat{y}_i -predicted value

 \bar{y}_i -Average of actual value

 R^2 -Model accuracy, ranging from zero to one, where a value close to 1 indicates a better fit and higher predictive accuracy

3. Results and Discussion

3.1 Analysis of TF and SR

All Data analysis was performed using the signal-to-noise (S/N) ratio from the Taguchi technique. Since both TF and SR need to be minimized, the smaller-the-better criterion was employed. The mathematical expression for the S/N ratio under the smaller-the-better is as given in Eq. (3).

$$\frac{s}{N} = -10\log\left[\frac{1}{n}(\sum y^2)\right] \tag{3}$$

where

n- Number of observations.

y- Observed value of TF and SR for ith observation.

Using Eq. (3), the S/N ratio for each experimental run was determined. The S/N ratio

Cite this article as:

^{*} Corresponding author.
E-mail address: velezhil07@gmail.com

analysis was used to assess the influence of input parameters on the output responses. Tables 3 and 4 present S/N ratio values for TF and SR, respectively. The results indicate that FR was the most significant parameter affecting TF, followed by DBD and SS. Conversely, DBD exhibits the greatest impact on SR, followed by FR and SS. ANOVA was used to identify the parameters significantly influencing the characteristics. It determines the importance of each parameter and its interaction by comparing the mean square values against estimated experimental errors at specific confidence levels. The percentage contribution quantifies the influence of each factor, calculated as the ratio sum of the squared deviations for each factor to the total sum of squared deviations. Tables 5 and 6 present the ANOVA results for the control factors influencing TF and SR during the drilling of the laminate. The ANOVA results, analysed at a 95% confidence level (p<0.05), revealed that FR and DBD were significant parameters influencing the drilling performance. The percentage contribution (PC) of FR and DBD for TF was 65.66% and 22.9%, respectively. Similarly, for SR, the PC of DBD and FR were 56.9% and 20.7%, respectively. The regression analysis has been developed to study the functional relationship between the responses and control variables. Multiple regression analysis was employed to establish the correlation between the responses and parameters. The regression equation for TF and SR was given in Eqs. (4) and Eq. (5), respectively. From these equations, the predicted R² values for TF and SR were 96.39% and 95.54%, respectively. These values indicate the strong predictive capability of the regression model and a high level of correlation between the parameters and responses.

Table 3. S/N ratio table for TF

Level	DBD (mm)	SS (rpm)	FR (mm/min)
1	-10.490	-11.143	-9.535
2	-11.562	-12.656	-11.696
3	-12.854	-11.106	-13.675
Delta	2.363	1.550	4.140
Rank	2	3	1

TF(kgf)=1.137+0.036*DBD+0.003853*SS+0.00 627*FR+0.0158(DBD*DBD)-0.00000(SS*SS) +0.000012(FR*FR)-0.000038(DBD*SS) +0.000147(DBD*FR) (4)

 $R^2 = 96.39\%$

Table 4. S/N ratio table for SR

	Level	DBD (mm)	SS (rpm)	FR (mm/min)
-	1	-16.37	-18.72	-16.92
	2	-17.84	-18.10	-17.90
	3	-19.55	-16.94	-18.94
_	Delta	3.18	1.78	2.01
	Rank	1	3	2

SR(μm)=1.166+0.264*DBD+0.001603*SS+0.0 1985*FR+0.06306(DBD*DBD)+0.000013(FR*F R)-0.000197(DBD*SS)-0.001620(DBD*FR) (5)

 $R^2 = 95.54\%$

Table 5. ANOVA table for TF

Source	DF	Adj SS	Adj MS	F-Value	P-Value
Model	9	22.1920	2.4658	155.14	0.000
Linear	3	19.4630	6.4877	408.19	0.000
A -DBD	1	4.7100	4.7100	296.35	0.000
B-SS	1	0.0027	0.0027	0.17	0.003
C-FR	1	14.7503	14.750	928.06	0.000
Square	3	2.6847	0.8949	56.31	0.000
DBD* DBD	1	0.0239	0.0239	1.50	0.002
SS * SS	1	2.6264	2.6264	165.25	0.000
FR * FR	1	0.0344	0.0344	2.16	0.160
2-Way Interaction	3	0.0443	0.0148	0.93	0.448
DBD*SS	1	0.0376	0.0376	2.36	0.015
DBD*FR	1	0.0066	0.0066	0.42	0.027
SS*FR	1	0.0001	0.0001	0.01	0.032
Error	17	0.2702	0.0159		
Total	26	22.4622			



Source	DF	Adj SS	Adj MS	F-Value	P-Valu
Model	9	65.8573	7.3175	927.86	0.000
Linear	3	63.3526	21.1175	2677.72	0.000
A -DBD	1	37.5556	37.5556	4762.08	0.000
B-SS	1	12.1032	12.1032	1534.70	0.000
C-FR	1	13.6939	13.6939	1736.40	0.000
Square	3	0.6764	0.2255	28.59	0.000
DBD* DBD	1	0.3817	0.3817	48.40	0.000
SS * SS	1	0.2508	0.2508	31.80	0.000
FR * FR	1	0.0439	0.0439	5.57	0.030
2-Way Interaction	3	1.8283	0.6094	77.27	0.000
DBD*SS	1	1.0208	1.0208	129.44	0.000
DBD*FR	1	0.8060	0.8060	102.20	0.000
SS*FR	1	0.0014	0.0014	0.18	0.678
Error	17	0.1341	0.0079		
Total	26	65.9914			

Table 7.	Prediction	results	for TF	and SR

S. No	DBD	SS	FR	TF (kgf)			S	R (µm)	
3. NO	טטט	აა	ГK	Predicted	Actual	Error	Predicted	Actual	Error
1	6	2220	80	2.65	2.7	1.85	4.97	5.71	4.6

Table 7 presents the predicted and actual results of TF and SR for the drilling of laminate. The optimal predicted and actual values for TF are 2.65 kgf and 2.7 kgf, respectively, while SR predicted and actual values are 4.97 μ m and 5.57%, respectively. The error percentages for TF and SR are calculated as 1.85% and 4.6%, respectively, indicating a close agreement between the model predictions and experimental observations. Figure 6 illustrates the comparison between the predicted and actual values of TF and SR at a 95% confidence level. The comparison underscores the accuracy and reliability of the predictive model in evaluating drilling performance metrics.

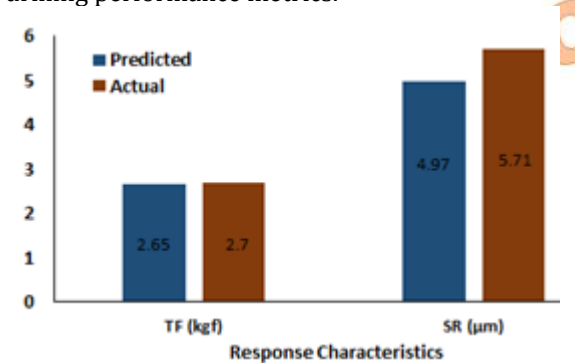


Fig. 6. Comparison plot for predicted and actual

3.2 Prediction of TF and SR using ANN

In this investigation, an ANN model for TF and SR was developed using the feedforward backpropagation technique.

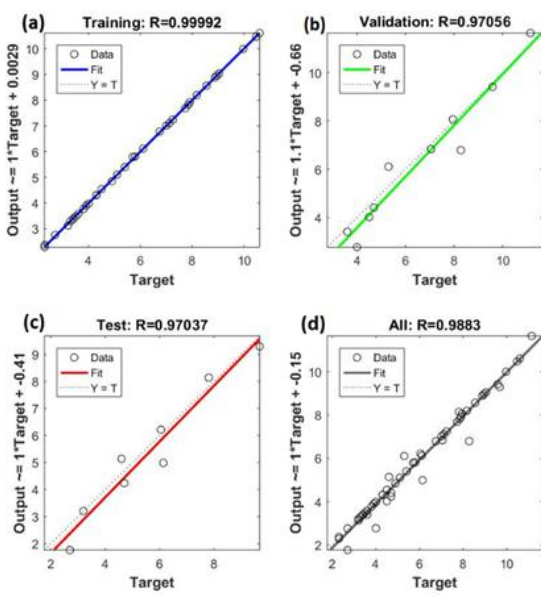


Fig. 7. ANN model results at training, testing, and validation.

The Levenberg-Marquard algorithm was employed to train, test, and validate the data obtained from the experimentation. After training the ANN model, the regression analysis was performed. The regression plot for training, testing, validation, and overall data showed a

coefficient correlation (R) of 0.9883, indicating strong agreement between predicted and actual experimental values, as illustrated in Fig. 7d.

Figure 7a illustrates the training input data for the ANN, where the dotted line represents the smooth fit, and the blue line indicates the direct fit. The ANN training is defined by the equation: projected value = 1 x Target value x 0.0029, indicating a strong correlation and optimal agreement between the experimental and predicted values. Figure 7b shows the validation data for ANN, where the inclined dotted and green line represents the smooth fit and direct fit, respectively. After the training and validation, the testing phase of the ANN was performed, as illustrated in Fig. 7c. Figure 8 shows the performance graph for the best prediction when the model was trained, tested, and validated. The selected ANN achieved a mean squared error (MSE) of approximately 0.089758 during the training phase at 2 epochs, with the training process converging after nearly 6 epochs. It was observed that TF and SR had a coefficient of determination (R2) of 96.39% and 95.54%, respectively, indicating that the model is highly adequate. Similarly, the correlation coefficient between the experiment and ANN ANN-predicted value was 0.98 for all training, testing, and validation phases, demonstrating the accurate prediction and strong predictive capability of the ANN model.

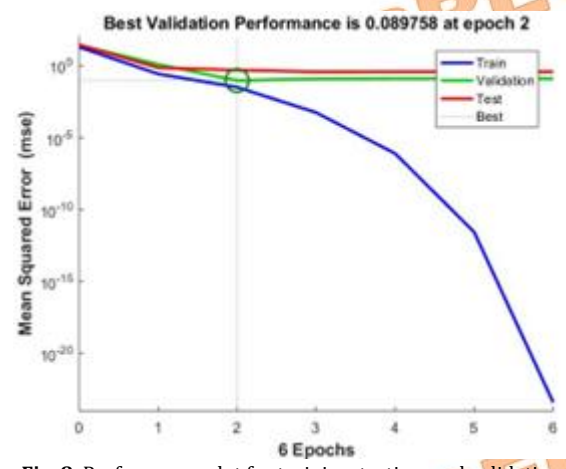


Fig. 8. Performance plot for training, testing, and validation

3.3. Effect of Drilling Parameters on TF and SR

Figure 9 illustrates that TF increases with a rise in DBD, SS, and FR, but decreases at higher SS values. The smaller DBD of 6mm typically results in lower TF, as it removes less material per revolution, requiring less force to penetrate the workpiece [16]. Conversely, a larger DBD of 10 mm requires a higher TF due to the increased volume of material removed per revolution. At an SS of 740 rpm, the drill bit rotates at a slower rate,

reducing cutting action and increasing contact time with the workpiece. This extended contact time facilitates more heat dissipation and potentially decreases friction. However, the prolonged interaction can lead to higher resistance, resulting in an increase in TF due to extended dwell time in the material [17].

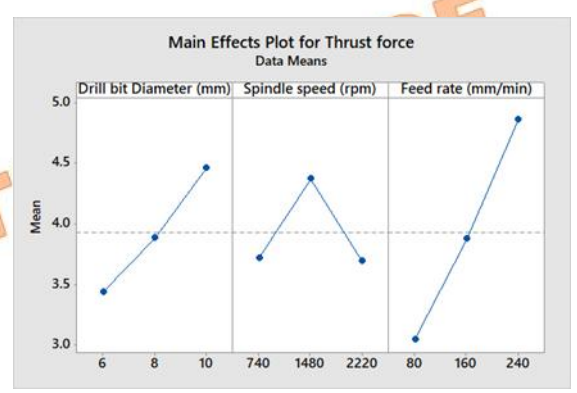


Fig. 9. Effect of drilling parameters on TF

At an SS of 1480 rpm, the drill bit achieves a moderate rotational velocity, facilitating efficient material removal with minimal dwell time. The SS of 2220 rpm results in rapid rotation, enabling high cutting velocities and efficient material removal rates. The rapid rotation reduces dwell time, minimizing frictional forces and potentially lowering the TF [18]. However, excessively high SS generates significant heat, which may cause defects such as melting or charring in the composite. The lower FR of 80 mm/min generally results in reduced TF due to less aggressive cutting action. The slower advancement allows for controlled chip formation and evacuation, reducing the risk of chip jamming and associated TF spikes. The drilling at FR of 160 mm/min results in moderate TF, balancing productivity with machining quality by ensuring efficient material removal, while maintaining control over chip formation and evacuation [19]. At a higher FR of 240 mm/min, the tool engages more material per unit of time, which speeds up material removal and increases resistance, resulting significant rise in TF. Additionally, increased heat and friction can lead to defects like melting or charring of the composite, which further contribute to increased TF drastically [20, 21]. Figure 10 illustrates the main effect plot for SR, revealing that SR increases with an increase in DBD and FR, but decreases as SS increases. At a DBD of 6 mm, the reduced cutting area in contact with the composite surface leads to limited cutting-edge engagement, with each cutting edge removing less material per revolution compared to a larger DBD. This localized cutting action can increase stresses and irregularities on the surface, resulting in higher SR [22]. At a DBD of 10mm, the increased surface area in contact with the

workpiece reduces friction and heat generation during drilling. The lower temperatures minimize material softening and the formation of defects [23], contributing to lower SR. As SS increases, SR decreases.

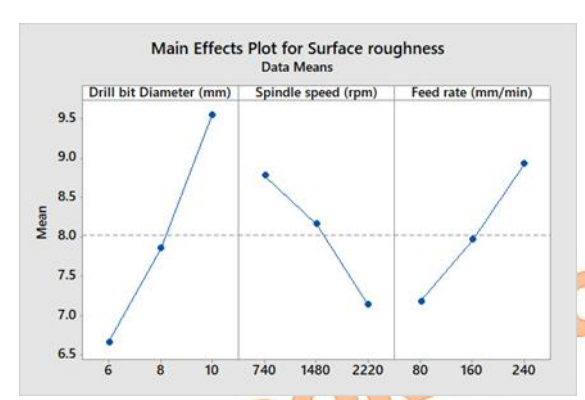


Fig. 10. Effect of drilling parameters on SR

At an SS of 2220 rpm, the drill bit rotates faster, reducing the contact time between the cutting edges and materials, which helps achieve smoother surface finishes by limiting the formation of defects. In contrast, at SS of 740 rpm, ineffective chip evacuation can lead to chip formation around the cutting edges, decreasing cutting efficiency and increasing SR.

At FR of 240 mm/min, a greater volume of material is removed per unit time, leading to increased cutting forces acting on the drill bit. These elevated forces can cause greater deformation and tearing of the material around the drilled hole, resulting in a higher SR [24]. Conversely, at FR of 80 mm/min, the prolonged contact times between the drill bit cutting edges and the material allow for more controlled and effective cutting action, leading to a smoother surface finish.

3.4. Microstructure Analysis

DBD has a significant impact on the surface morphology of the drilled composite. At a DBD of 6 mm, high stress concentration occurs at the cutting interface, which promotes the formation of finer and more precise holes [25]. However, this can also increase the likelihood of fiber pullout, as illustrated in Fig. 11(a). In contrast, at a DBD of 10 mm, the increased frictional heat generated in the drilling zone results in a more robust hole structure. However, this also increases the risk of thermal breakdown and delamination of the laminate, as shown in Fig. 11(b). At an SS of 740 rpm, reduced heat generation leads to defects and fiber pull-out, resulting in higher SR. Increasing the SS to 1480 rpm reduces SR and strikes a balance between minimizing thermal impact and producing sufficient heat for a cleaner cut. However, at SS of 2220 rpm, the increased frictional heat facilitates smoother and more precise cuts but risks matrix degradation and matrix debonding [26], as depicted in Fig. 12.

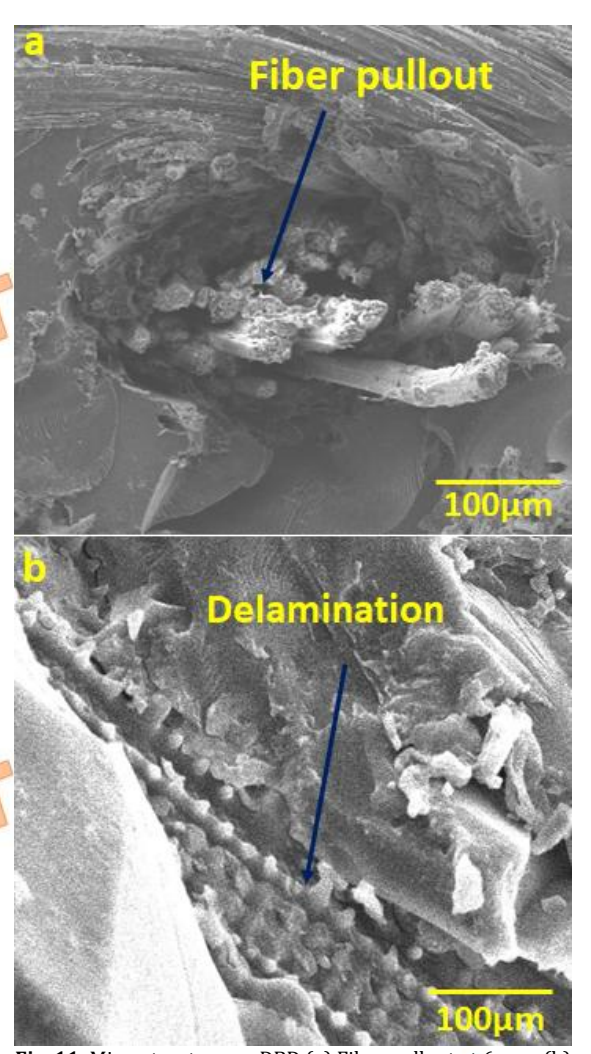


Fig. 11. Microstructure on DBD (a) Fiber pullout at 6 mm, (b) delamination at 10 mm

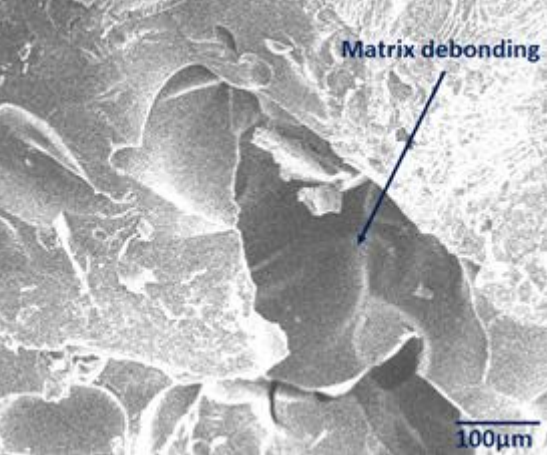


Fig. 12. Microstructure on SS Matrix debonding at 2220 rpm

While the higher heat generation improves cutting quality, it may still thermally deteriorate the matrix. Therefore, an SS of 1480 rpm efficiently reduces SR while preserving the

microstructural integrity [27]. At an FR of 80 mm/min, the drilling process is efficient, leading to reduced stress on the material and a smoother surface morphology with fewer defects, such as matrix cracking, as shown in Fig. 13(a). However, the lower FR may exacerbate thermal impacts, potentially leading to heat-induced materials deterioration [28]. When the FR is increased to 160 mm/min, a higher level of impact stress is introduced. causing more noticeable microstructural changes, such as matrix deformation, as seen in Fig. 13(b). At the maximum FR of 240 mm/min, the drilling becomes significantly more aggressive, resulting in severe impact stress and rapid material ablation. This intense drilling action leads to delamination [29], matrix cracking, and extensive fiber damage [30], which increases SR.

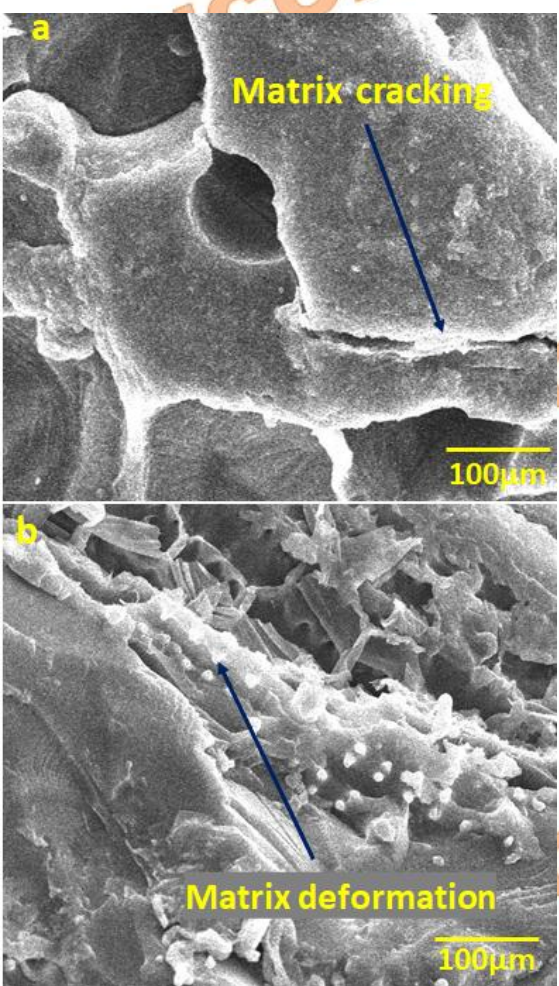


Fig. 13. Microstructure on FR (a) Matrix cracking at 80 mm/min, (b) Matrix deformation at 160 mm/min

4. Conclusions

This investigation explored the prediction and optimization of drilling characteristics, such as TF and SR, using an integrated Taguchi and ANN approach. The epoxy resin-based hybrid composite reinforced with natural fibers was fabricated using the hand lay-up technique.

ANOVA with the smaller-the-better criterion was applied to identify the significant parameters. An ANN model was developed using a feedforward backpropagation algorithm to predict the responses. The study examined the effects of DBD, SS, and FR on TF and SR. Based on the results observed from the Taguchi and ANN models, the following conclusions were drawn.

The ANOVA results indicated that the parameters had a significant effect on both TF and SR at a 95% confidence level (p<0.05). The regression coefficient (R²) for TF and SR were 96.39% and 95.54%, respectively, demonstrating a strong correlation between the parameters and the responses.

The FR and DBD were identified as the most significant parameters influencing TF, with their respective contributions being 65.66% and 22.9%, respectively. Similarly, SR, DBD, and FR contributed 56.9% and 20.7%, respectively.

The coefficient of correlation (R) of 0.9883 was achieved during the training, testing, and validation phases of the ANN model, indicating a good agreement between the predicted and actual experimental values. The proposed ANN model attained an MSE of approximately 0.089758 during the testing phase after 2 epochs, demonstrating its high prediction accuracy.

The main effect plots showed that both TF and SR increased with an increase in DBD and FR, while they decreased as SS increased. The predicted TF and SR values were 2.65 kgf and 4.97 μ m, respectively, at the optimal conditions of 6 mm DBD, 2220 rpm SS, and 80 mm/min FR. The error between the actual and predicted values during the optimization of TF and SR was 1.85% and 4.6%, respectively.

SEM analysis revealed the formation of fiber pullout and delamination at varying DBD of 6 mm and 10 mm, respectively. Additionally, matrix cracking and matrix deformation were observed at FR of 80 mm/min and 160 mm/min, respectively.

It was concluded that Taguchi, combined with the ANN approach, demonstrated strong effectiveness, significantly improving the prediction accuracy for both TF and SR. This hybrid method offered enhanced performance by optimizing parameters and accurately predicting the drilling characteristics of the composite laminate.

In order to improve predictive modeling and practical applicability, further study may examine the effects of various resin systems, tool geometries, and fiber combinations on drilling. Additionally, real-time monitoring and advanced machine learning may be integrated.

Conflicts of Interest

The author declares that there is no conflict of interest regarding the publication of this article.

Funding statement

No financial support was received from public, private, or nonprofit organizations for this study.

References

- [1]. Das, T.K., Ghosh, P. and Das, N.C., 2019. Preparation, development, outcomes, and application versatility of carbon fiber-based polymer composites: a review. *Advanced Composites and Hybrid Materials*, 2(2), pp. 214–233.
- [2]. Feng, Y., Hao, H., Lu, H., Chow, C.L. and Lau, D., 2024. Exploring the development and applications of sustainable natural fiber composites: a review from a nanoscale perspective. *Composites Part B: Engineering*, pp. 111369.
- [3]. Kasirajan, S., Umapathy, D., Chandrasekar, C., Aafrin, V., Jenitapeter, M., Udhyasooriyan, L. and Muthusamy, S., 2019. Preparation of poly(lactic acid) from Prosopis juliflora and incorporation of chitosan for packaging applications. *Journal of Bioscience and Bioengineering*, 128, pp. 323–331.
- [4]. Rajan, B.S., Balaji, M.S. and Saravanakumar, S.S., 2018. Effect of chemical treatment and fiber loading on physico-mechanical properties of Prosopis juliflora fiber-reinforced hybrid friction composite. *Materials Research Express*, 6, pp. 035302.
- [5]. Kuntoğlu, M. and Sağlam, H., 2019. Investigation of progressive tool wear for determining optimized machining parameters in turning. *Measurement*, 140, pp. 427–436.
- [6]. Rajamurugan, T.V., Shanmugam, K. and Palanikumar, K., 2013. Analysis of delamination in drilling glass fiberreinforced polyester composites. *Materials & Design*, 45, pp. 80–87.
- [7]. Ganesan, V., Shanmugam, V., Alagumalai, V., Kaliyamoorthy, B., Das, O. and Misra, M., 2024. Optimisation of mechanical behaviour of Calotropis gigantea and Prosopis juliflora natural fibre-based hybrid composites by using Taguchigrey relational analysis. *Composites Part C: Open Access*, 13, pp. 100433.
- [8]. Raja, T., Devarajan, Y., Dhanraj, G., Pandiaraj, S., Rahaman, M. and Thiruvengadam, M., 2024. Delamination analysis of drilling parameters on neem/banyan fiber-reinforced sawdust

- particulates hybrid polymer composite. *Biomass Conversion and Biorefinery*, 14, pp. 10747–10757.
- [9]. Lilly Mercy, J., Shaqir Tanvir, M. and Swaroopkanth, K., 2017. Experimental investigation and Taguchi optimisation of drilling properties on teak wood reinforced epoxy resin. Materials Science and Engineering Conference Series, 197, pp. 012063.
- [10]. Mohan Kumar, A., Rajasekar, R., Manoj Kumar, P., Parameshwaran, R., Karthick, A., Mohanavel, V. and Muhibbullah, M., 2021. Investigation of drilling process parameters of palmyra-based composite. *Advances in Materials Science and Engineering*, 2021, pp. 4222344.
- [11]. Rajaraman, G., Agasti, S.K. and Jenarthanan, M.P., 2020. Investigation on effect of process parameters on delamination during drilling of kenafbanana fiber reinforced epoxy hybrid composite using Taguchi method. *Polymer Composites*, 41, pp. 994–1002.
- [12]. Boga, C. and Koroglu, T., 2021. Proper estimation of surface roughness using hybrid intelligence based on artificial neural network and genetic algorithm. *Journal of Manufacturing Processes*, 70, pp. 560-569.
- [13]. Bolat, Ç., Özdoğan, N., Çoban, S., Ergene, B., Akgün, İ.C. and Gökşenli, A., 2024. Estimation of cutting forces in CNC slot-milling of low-cost clay reinforced syntactic metal foams by artificial neural network modeling. Multidiscipline *Modeling in Materials and Structures*, 20(3), pp. 417-436.
- [14]. Elaiyarasan, U., Ananthi, N. and Sathiyamurthy, S., 2024. Prediction and parametric effect of electrical discharge layering of AZ31B magnesium alloy using response surface methodology-assisted artificial neural network. *Bulletin of Materials Science*, 47(2), pp. 109.
- [15]. Elaiyarasan, U., Satheeshkumar, V., Senthilkumar, C. and Nandakumar, C., 2022. Mathematical and artificial neural network model in composite electrode assisted electrical discharge coating. Surface Topography: Metrology and Properties, 10(2), pp. 025004.
- [16]. Mohan, N.S., Ramachandra, A. and Kulkarni, S.M., 2005. Machining of fiberreinforced thermoplastics: influence of feed and drill size on thrust force and torque during drilling. *Journal of Reinforced Plastics and Composites*, 24, pp. 1247–1257.

- [17]. Yu, Z., Li, C., Kurniawan, R., Park, K.M. and Ko, T.J., 2019. Drill bit with a helical groove edge for clean drilling of carbon fiber-reinforced plastic. *Journal of Materials Processing Technology*, 274, pp. 116291.
- [18]. Rajamurugan, T.V., Shanmugam, K., Rajakumar, S. and Palanikumar, K., 2012. Modelling and analysis of thrust force in drilling of GFRP composites using response surface methodology (RSM). *Procedia Engineering*, 38, pp.3757–3768.
- [19]. Rao, Y.S., Mohan, N.S., Shetty, N. and Acharya, S., 2023. Drilling response of carbon fabric/solid lubricant filler/epoxy hybrid composites: an experimental investigation. *Journal of Composites Science*, 7, pp. 46.
- [20]. Prakash, R. and Krishnaraj, V., 2021. Cutting tools for machining composites. In: Advances in Machining of Composite Materials: Conventional and Non-Conventional Processes. Springer International Publishing, Cham, pp. 485– 515.
- [21]. Yalçın, B., Bolat, Ç., Ergene, B., Karakılınç, U., Yavaş, Ç., Öz, Y., Ercetin, A., Maraş, S. and Der, O., 2024. Effect of drilling parameters and tool diameter on delamination and thrust force in the drilling of high-performance glass/epoxy composites for aerospace structures with a new design drill. *Polymers*, 16(21), pp. 3011.
- [22]. Bolat, Ç., Karakılınç, U., Yalçın, B., Öz, Y., Yavaş, Ç., Ergene, B., Ercetin, A. and Akkoyun, F., 2023. Effect of drilling parameters and tool geometry on the thrust force and surface roughness of aerospace grade laminate composites. *Micromachines*, 14(7), pp. 1427.
- [23]. Lazar, M.B. and Xirouchakis, P., 2011. Experimental analysis of drilling fiber reinforced composites. International Journal of Machine Tools and Manufacture, 51, pp. 937–946.
- [24]. Rajamurugan, T.V., Rajaganapathy, C., Jani, S.P., Gurram, C.S., Allasi, H.L. and [31].

- Damtew, S.Z., 2022. Analysis of drilling of coir fiber-reinforced polyester composites using multifaceted drill bit. *Advances in Materials Science and Engineering*, 2022, pp. 9481566.
- [25]. Rao, Y.S., Mohan, N.S., Shetty, N. and Shivamurthy, B., 2019. Drilling and structural property study of multilayered fiber and fabric reinforced polymer composite: a review. *Materials and Manufacturing Processes*, 34, pp. 1549–1579.
- [26] Mohan Kumar, A., Rajasekar, R., Manoj Kumar, P., Parameshwaran, R., Karthick, A. and Muhibbullah, M., 2021. Comparative analysis of drilling behaviour of synthetic and natural fiberbased composites. *Advances in Materials Science and Engineering*, 2021, pp. 9019334.
- [27]. Franz, G., Vantomme, P. and Hassan, M.H., 2022. A review on drilling of multilayer fiber-reinforced polymer composites and aluminum stacks: optimization of strategies for improving the drilling performance of aerospace assemblies. *Fibers*, 10, pp. 78.
- [28]. Xu, J., Geier, N., Shen, J., Krishnaraj, V. and Samsudeensadham, S., 2023. A review on CFRP drilling: fundamental mechanisms, damage issues, and approaches toward high-quality drilling. *Journal of Materials Research and Technology*, 24, pp.9677–9707.
- [29]. Ergene, B., Bolat, C., Karakilinc, U. and Irez, A.B., 2023. A comprehensive investigation of drilling performance of anisotropic stacked glass-carbon fiber reinforced hybrid laminate composites. *Polymer Composites*, 44(5), pp. 2656-2670.
- [30]. Rathod, D., Rathod, M., Patel, R., Shahabaz, S.M., Shetty, S.D. and Shetty, N., 2021. A review on strengthening, delamination formation, and suppression techniques during drilling of CFRP composites. *Cogent Engineering*, 8, pp. 1941588.